

Labeling the Pulmonary Arterial Tree in CT Images for Automatic Quantification of Pulmonary Embolism

Ralph J.M. Peters^{ab}, Henk A. Marquering^a, Halil Doğan^c, Emile A. Hendriks^b, Albert de Roos^c,
Johan H.C. Reiber^a, Berend C. Stoel^a

^aDivision of Image Processing, Department of Radiology, Leiden University Medical Center,
Leiden, The Netherlands;

^bInformation and Communication Theory Group, Delft University of Technology, Delft, The
Netherlands;

^cDepartment of Radiology, Leiden University Medical Center, Leiden, The Netherlands.

ABSTRACT

Contrast-enhanced CT Angiography has become an accepted diagnostic tool for detecting Pulmonary Embolism (PE). The CT obstruction index proposed by Qanadli, which is based on the number of obstructed arterial segments, enables the quantification of PE severity. Because the required manual identification of twenty arterial segments is time consuming, we propose a method for automated labeling of the pulmonary arterial tree to identify the arterial segments. Assuming that the peripheral parts of the arterial tree contain most relevant information for labeling, we propose a bottom-up labeling algorithm exploiting the spatial information of the peripheral arteries. A model of reference positions of the arterial segments was trained using manually labeled trees of 9 patients. To improve accuracy, the arterial tree was partitioned into sub-trees enabling an iterative labeling technique that labels each sub-tree separately. The accuracy of the labeling technique was evaluated using manually labeled trees of 10 patients. Initially an accuracy of 74% was obtained, whereas the iterative approach improved accuracy to 85%. The labeling errors had minor effects on the calculated Qanadli index. Therefore, the presented labeling approach is applicable in automated PE quantification.

Keywords: Quantitative image analysis, X-ray CT, detection, risk assessment

1. INTRODUCTION

Pulmonary Embolism (PE) is the obstruction of an artery in the lungs, mostly caused by blood clots from peripheral veins. As a result, a part of a lung is not perfused. PE is the third most common acute cardiovascular disease in western population, after myocardial infarction and stroke. Prompt treatment with anti-coagulants is essential to prevent loss of life, therefore early diagnosis is critical.

Contrast-enhanced CT Angiography is nowadays the first-line diagnostic tool for patients with suspected acute PE [1]. In these images, emboli are expressed as dark spots inside bright vessels, as indicated in Fig. 1. Qanadli *et al.* [2] proposed a semi-quantitative CT obstruction index and Wu *et al.* [3] successfully related this index to patient outcome. For the calculation of the Qanadli index the correct identification of the 20 arterial segments (based upon the nomenclature of Remy-Jardin *et al.* [6]) is required. This approach requires a time consuming determination of the number of occluded arterial segments and identification of 20 arterial segments. The manual quantification using the Qanadli index commonly takes 5 to 10 minutes, but in some cases 25 minutes. Therefore, we present an algorithm to automatically identify the segmental branches by labeling the pulmonary arterial tree, which can be used for future automatic PE quantification using the Qanadli index.

To our knowledge, no approaches have been reported previously to automate the quantification of PE based on the Qanadli index. A few approaches have been reported that (semi) automatically detect the position of pulmonary emboli [11;12]. Furthermore, a wide variety of automated pulmonary vascular tree segmentation techniques exists [12;13]. However, automatic identification of the arterial segmental branches has not been covered yet. Automated PE quantification based on this index requires an automated PE detection, the quantification of the degree of obstruction, and the determination of the number of arterial segments distal to the occlusion. To perform this last step, arterial tree

segmentation and arterial tree segment labeling is necessary. Figure 2 shows an overview of such an approach for the automated quantification of PE.

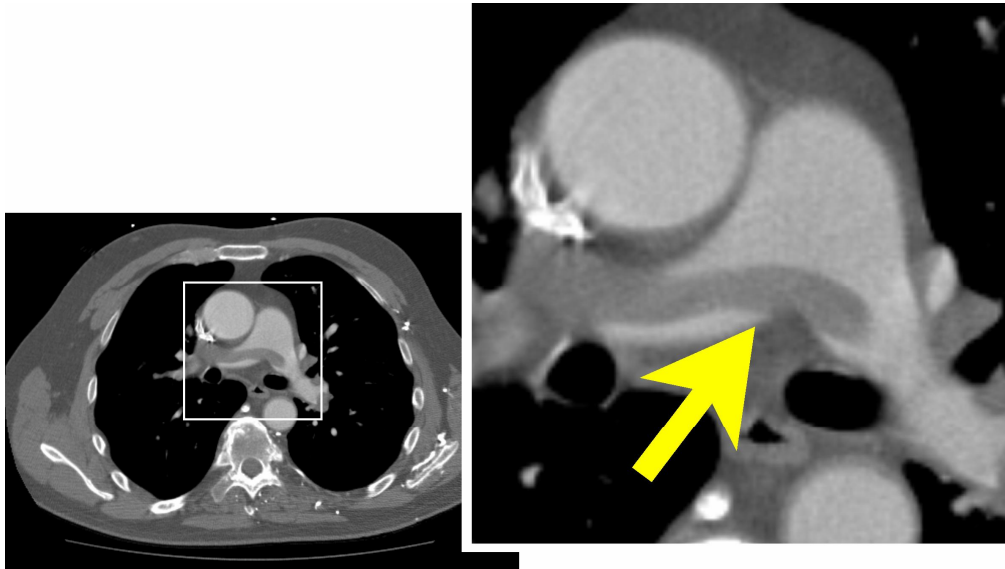


Fig. 1: CTA axial slice showing a pulmonary embolus (dark spot) inside the pulmonary trunk (bright structure).

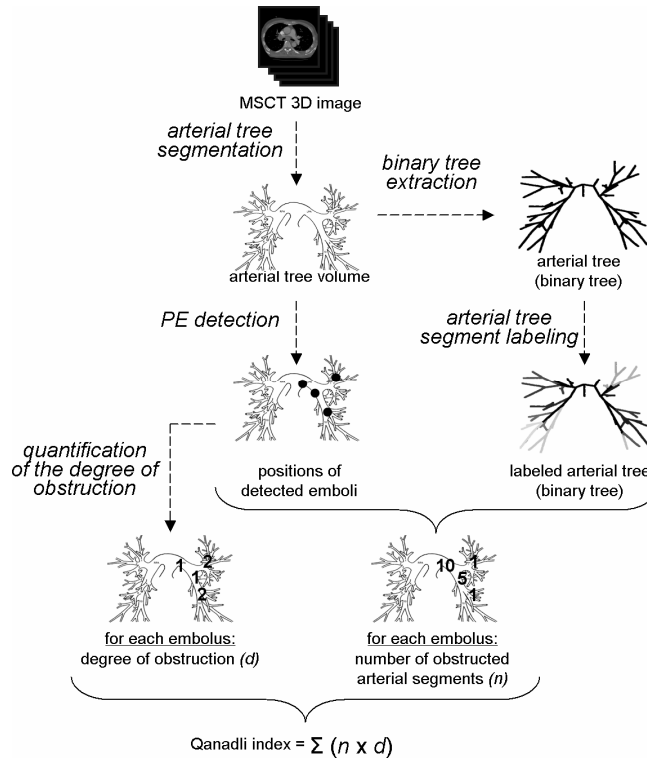


Fig. 2. Required steps to automate quantification of PE based on the Qanadli index. The first step is to produce a segmented arterial tree. In this volume the positions and size of the emboli can be detected. This paper focuses on the right part of the figure: the binary tree representation of a segmented arterial tree volume is used to label the tree. With the labeled tree, the position of a detected embolus can be used to determine the number of obstructed arterial segments. Finally the Qanadli index is calculated using the severity and number of obstructed arterial segments for each embolus.

In this paper, we present an algorithm to identify the segmental branches by labeling the pulmonary arterial tree, which is required for the automated quantification of PE using the Qanadli index. Related work in the area of PE detection, vascular tree segmentation and tree labeling is described in Section 2. In Section 3, we describe the labeling algorithm and the validation method. The results are presented in Section 4, followed by a discussion of these results in Section 5 and the conclusions in Section 6.

2. RELATED WORK

For the automatic detection of pulmonary emboli in CTA images, Masutani *et al.* [9] reported a method that analyses features inside a segmented volume of pulmonary vessels. These features include vascular size, local contrast, degree of curvilinearity based on second derivatives, and geometric features such as volume and length. Bouma *et al.* [10] proposed some additional PE detection features based on intensity and shape. An automated visualization method has been proposed by Pichon *et al.* [11] to assist radiologists by highlighting potential emboli on a 3D representation of the pulmonary arterial tree. After segmentation of the lung vessels, a shaded surface display is created from the segmented vessel tree volume, where the outside colors are based on density values inside the vessels.

Segmenting the arterial tree is an important preprocessing step before the labeling of the arterial tree to identify the segmental branches can be carried out. Vessel segmentation techniques are widely documented [12]. Some automated methods to segment the pulmonary vascular tree structures are reported by Masutani *et al.* [9] and Sebbe *et al.* [13]. Kiraly *et al.* [14] describe a method to segment occluded arteries from CT images and estimate the affected lung volume from the position of an embolus in the arterial tree. Automated pulmonary vascular tree segmentation methods commonly have difficulties in excluding the venous tree. Sonnemans [15] reports that this is caused by similar brightness, streak artifacts, flow voids, pulmonary emboli causing filling defects and seemingly touching vessels due to motion blurring. To prevent false detection of emboli in the veins, Sonnemans proposed a classifier based on the first eigenvalue of the Hessian matrix. Evaluation showed that to this moment the sensitivity and specificity were too low to achieve a robust segmentation.

With the segmented pulmonary arteries and the detected emboli, automatic quantification of PE may become feasible. However, PE quantification using the Qanadli index also requires pulmonary arterial tree labeling, which is the focus of this paper. Pisupati *et al.* present a tracking algorithm [16] to match pulmonary tree structures using central axis tree representations [17]. The tracking algorithm results in an accurate match on various airway CT data sets of the same dog lung under different (simulated) breath hold positions. However, we expect that this tracking method would fail in matching arterial trees of different human individuals. The algorithm proposed by Pisupati *et al.* starts by mapping the tree root and recursively matching children nodes. Such a topology-preserving algorithm is not suitable for labeling multiple arterial trees because of the differences in branch topology between individuals. The order of branching of the various arterial segments may vary between patients. It has been suggested [18] that the Horton-Strahler index [19;20] can be used for the classification of pulmonary arteries. This index is able to group topological self-similar branching structures; root nodes of similar trees are assigned to similar values. However, because the arterial pulmonary tree structures show significant variations in topology, we chose not to use this Horton-Strahler index for labeling.

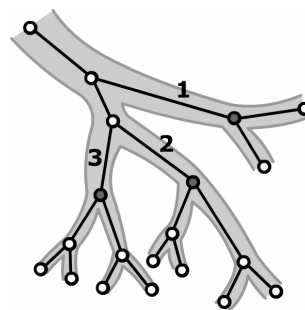


Fig. 3. Schematic representation of the arterial tree segments 1-3 with the corresponding binary representation; vertices represent artery branches, white and gray nodes represent bifurcations, the gray nodes indicate the position of the segment root bifurcations

3. METHODS

The nomenclature of the pulmonary arterial tree is based on the positions of the peripheral parts of the arterial tree (e.g. apical, anterior, lateral basal). Therefore, our hypothesis is that the positions of the peripheral parts produce more useful information than positions of its root. We developed a bottom-up algorithm that labels the arterial tree starting at the peripheral parts of the tree. For this purpose, we represented the arterial tree by a binary tree in which each node corresponds to a bifurcation, and each vertex to a branch (see Fig. 3). First, we present the bottom-up algorithm that labels the arterial tree starting at the peripheral parts of the tree. This method uses a set of reference positions that represents the peripheral locations of the arterial segments. Second, we present the method that determines this set of reference positions using manually labeled arterial trees.

3.1 Pulmonary artery tree labeling

The labeling algorithm matches the binary tree representation of the pulmonary artery tree with a model that contains a set of reference positions that represents the peripheral locations of the arterial segments. The tree-labeling algorithm is described in the following steps (see Figure 4):

- Construct a binary tree that has to be labeled, and include a pre-defined model with a set of reference positions.
- Scale the reference positions to match the volume of the unlabeled tree.
- For each reference position, find the nearest tree node and assign its label.
- Assigned the label to all parent nodes. A node is classified as a 'branch origin node' if (1) its parent node has been assigned more than one label and (2) all possible children nodes have one or no label.
- For each of these 'branch origin nodes', the label is assigned to all child nodes.

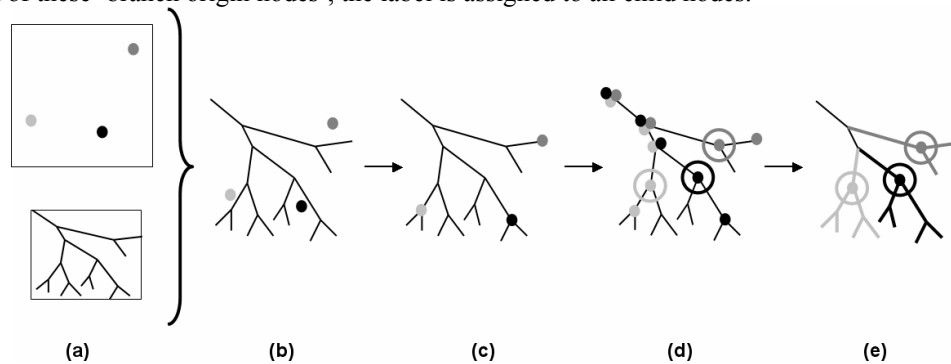


Fig. 4. Tree labeling algorithm: for each reference position, a label is assigned to its nearest node; subsequently labels are assigned to their parents nodes and branch origin node positions are deduced to label the complete tree

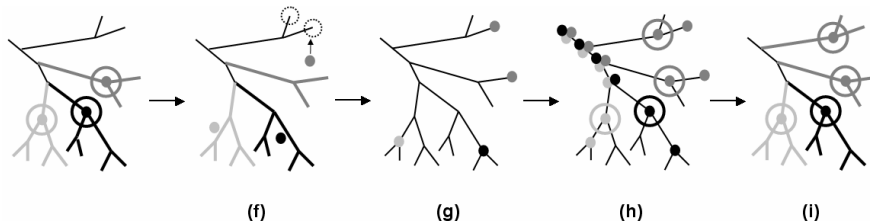


Fig. 5. The revisit step in the tree labeling algorithm: labels are assigned to unlabeled leaf nodes that lie closest to reference position; subsequently labels are assigned to their parent nodes and branch origin node positions are deduced to label the complete tree

As a segment can have more than one segmental branch origins, some tree structures remain unlabeled after the approach described above. These segments are labeled in the following revisit step (Fig.5).

- Select the unlabeled leaf node that lies closest to a reference position.
- Add this node to the list of selected nodes found in step c.

- h. Perform step d.
- i. Perform step e.

3.2 Iterative labeling of the arterial tree

In order to increase the robustness against anatomical variations we implemented an iterative labeling approach to label a number of arterial sub-trees. For example, we may separately label the arterial tree in the left and right lung. In this approach we start with determining only two reference positions for the left and right arterial tree. These reference positions are used to separate the left and right arterial tree. Subsequently, in each of the two sub-trees, reference positions are used to label the arterial segments 1 to 10. The iterative labeling by grouping segments is successful if the labeled branches in the specific group have a common trunk. For example, the left arterial segments all share one common trunk. Fig. 6 shows a schematic overview of this iterative labeling.

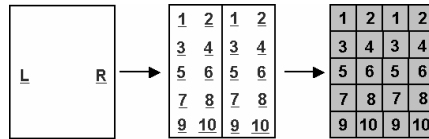


Fig. 6. Labeling left and right tree iteratively (basic approach); 2 reference positions are placed to separate the left and right tree; then 10 reference positions are placed to label each side of the tree; the labeled segments are indicated as gray areas.

Generally, the lower arterial segments 7, 8, 9, and 10 show more variation in size and position. However, the topology for these segments is similar in most cases. Segments 7, 8, 9 and 10, the lower anterior segments 7 and 8, and the lower posterior segments 9 and 10 commonly have a single common trunk [6]. Fig. 7 shows the multi-phase iterative labeling.

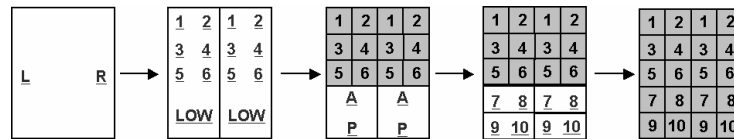


Fig. 7. Labeling the lower segments iteratively as well (multi-phase approach); after separating the left and right tree; the lower segments 7-10, the lower anterior (A) segments 7-8, and lower posterior (P) segments 9-10 are all labeled separately.

3.3 Determining reference positions

To determine the reference positions for the labeling algorithm we used manually labeled bifurcation positions in the peripheral parts of the tree. This approach is illustrated in Fig. 8 and described below.

- a. Construct a set of manually labeled binary trees in which a vertex contains the position and the label of the pulmonary segment.
- b. Normalize each labeled tree based on the minimal rectangular volume containing the binary tree.
- c. Construct a 3D matrix for each tree in which every position is labeled according to the closest vertex.
- d. Deduce a single matrix from a set of matrices, for every label, in which each position contains the incidence of the label on that position. Subsequently, determine the segment reference positions by the center of gravity calculation of the volume with the highest incidence.

For every position in the volume, the number of segment labels of multiple volumes is counted. The result is schematically shown as different areas in Fig. 8, where dark colors represent sub-volumes with high incidence of the particular label. The segment reference position is determined by the calculation of the center of gravity of the sub-volume having the highest incidence. The reference positions have to be calculated using a discretized grid. The size of the grid is 20x20x20 voxels when not stated otherwise.

Note that the determination of the reference positions has to be carried out only once.

3.4 Calculating the Qanadli index

Once the binary tree has been labeled, the Qanadli index may be determined. This index is defined as $\Sigma (n \times d)$ over all 20 arterial segments, with n the number of segmental branches arising distally, and d the degree of obstruction as partial obstruction ($d = 1$) or total obstruction ($d = 2$). Isolated subsegmental emboli are considered as a partial segmental

occlusion ($d = 1$). The percentage of vascular obstruction is obtained by dividing the index by the maximum score of 40 and multiplying the result by 100 [3].

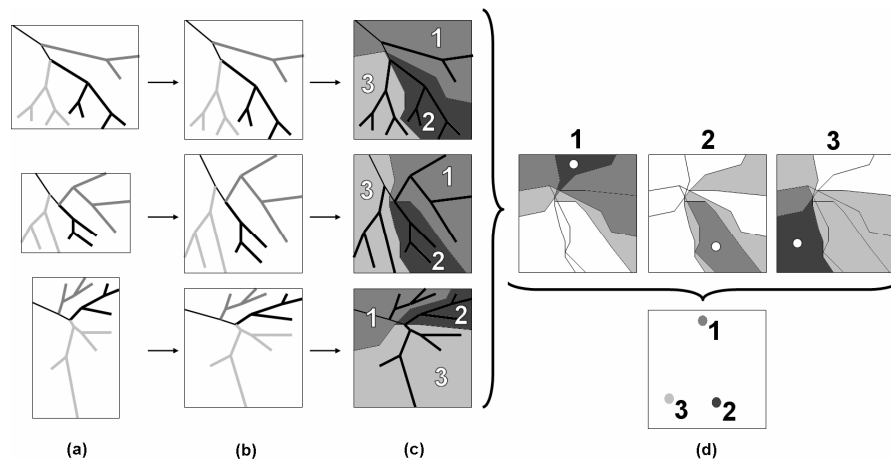


Fig. 8: Determining the reference positions from labeled data: each labeled tree is scaled; every position in the volume is labeled according to the closest labeled tree vertex; reference positions are extracted by finding the center of gravity of the sub-volume having the highest incidence.

To calculate the Qanadli index, the degree of obstruction of each embolus is visually graded for all occluded arterial segments. For each visually detected embolus position, the corresponding vertex in the binary tree representation is identified. The distal node of this vertex is used for examining the labels of the parent and children nodes. We deduce the list of occluded arterial segments from the labels of the children nodes. In case only one occluded arterial segment is found, we defined the embolism as segmental, subsegmental or peripheral using the labels of the parent nodes. The highest degree of segmental obstruction (0, 1 or 2) determines the score of each arterial segment. If no segmental obstruction is found, the highest degree of subsegmental obstruction (0 or 1) is used.

With this scheme, we are able to calculate the Qanadli index using a labeled binary tree and the visually extracted emboli positions with the corresponding degrees of obstruction (partial or total).

3.5 Validation

The labeling as proposed here contains two possible sources of error: errors due to the labeling method itself, and imperfections in the position of the reference points. To separately validate the labeling approach, we perform the labeling using “ideal” reference positions. For this test we use reference positions obtained from the current dataset itself.

To validate the labeling approach including the determination of reference positions, we perform leave-one-out tests. In this approach we determine reference positions using 9 labeled datasets. The remaining dataset is subsequently labeled using this set of reference positions.

The accuracy of the labeling procedure is determined by comparing the results with the manual labeling. The labeling accuracy of single arterial tree segments is defined as the ratio of correctly labeled nodes and the total number of nodes of this segment. The labeling accuracy of the complete arterial tree is defined as the average accuracy of the twenty segments. The automatic determined Qanadli index is compared with values determined with the manually labeled trees.

3.6 Peripheral branches

To test our hypothesis that most information for labeling the arterial tree can be found in peripheral parts of the tree, we perform tests using truncated trees. To study the effect including peripheral parts of the arterial trees on the labeling accuracy, all peripheral branches arising from the subsegmental branches were removed from the binary trees. We test this by using “ideal” reference positions obtained from the current dataset itself to evaluate its effect on the labeling. Furthermore, we performed leave-one-out tests to include the effect on the determination of the reference positions.

3.7 Data acquisition

We used CTA images of 10 patients with clinical suspicion of acute PE (7 men, 3 women; age range, 19-76 years). These images were acquired by standard contrast enhanced (Xenetix 300) multi-detector computed tomography using a

Toshiba Aquilion 16CFX 16-slice MDCT scanner. Acquisitions of 0.5 or 1 mm sections of the entire chest were performed during a single breath-hold, with a scan time of 12 seconds or less. The rotation time was 0.4 s, the pitch factor 1.4, the tube current was 250-300 mA, and the tube voltage 100 kV. 100 ml of contrast agent was injected with a double barrel power injector (Medrad, Pittsburgh, PA) in the antecubital vein with an injection rate of 4.0 ml/sec. The acquisition of the pulmonary angiography scan was started after automated threshold enhancement detection in the pulmonary trunk. A difference of 100 Hounsfield units was selected as a threshold for starting the acquisition. The effective radiation dose varied between 2.8-3.9 mSv.

Binary tree representations of the pulmonary arterial trees were extracted manually by selecting positions of bifurcations in the CTA images. We labeled our data by selecting nodes (visualized in the CTA image) that corresponded to the arterial segmental branch origins, based on the standard nomenclature and descriptions of Remy-Jardin *et al.* [6].

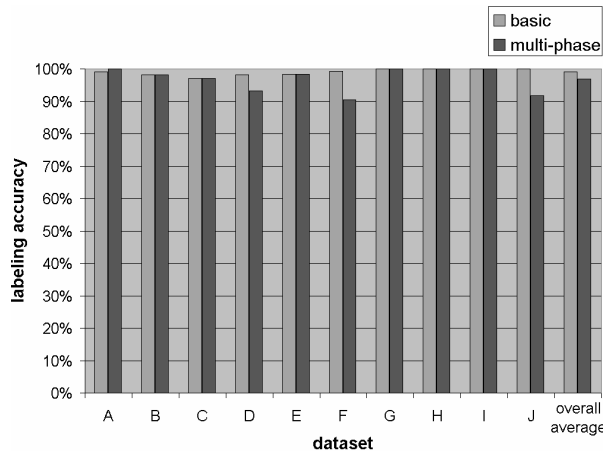


Fig. 9: labeling accuracy using “ideal” reference positions; the bars show the labeling accuracies for each test; the bars in the last column show the overall average accuracy for all 10 datasets

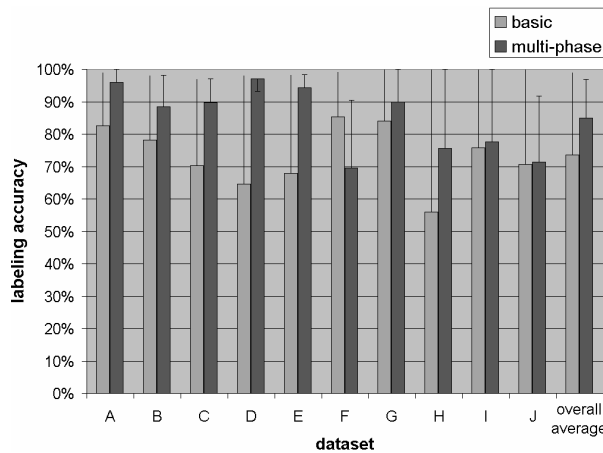


Fig. 10: labeling accuracy using leave-one-out tests (included searching and labeling of unlabeled parts of the tree); the black lines refer to the best possible accuracy that was shown in Fig. 9

4. RESULTS

The accuracy of the proposed approaches was studied with leave-one-out analysis using manually labeled pulmonary trees of 10 patients with clinical suspicion of acute PE.

4.1 Labeling results

Our proposed method contains two possible sources of error: inaccuracies of the labeling method and imperfections in the reference positions. To separately validate the labeling method, we performed the labeling using “ideal” reference

positions. The ideal reference positions were determined using manually labeled positions from the same dataset only. Fig. 9 shows the labeling accuracy of this approach of the basic and multi-phase labeling method. The basic approach results in an accuracy of 73.5% (with a standard deviation of 8.9%), the multi-phase method results in an accuracy of 84.9% (with a standard deviation of 10.4%).

4.2 Peripheral branches

Regarding our hypothesis that most information for labeling the arterial tree can be found in the peripheral parts of the tree, we present accuracy results with truncated trees. Fig. 11 shows the average percentages correctly labeled nodes per segments if all peripheral branches arising from the subsegmental branches were removed.

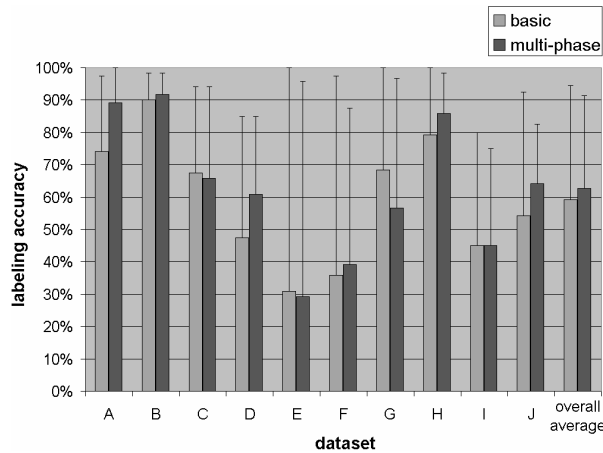


Fig. 11: labeling accuracy using leave-one-out tests on truncated tree datasets (included search and label unlabeled parts of the tree), the black lines refer to the best possible accuracy when “ideal” reference positions are used for these truncated trees.

4.3 The Qanadli index

As the final step of the validation, we present the automatically determined Qanadli indices to study the accuracy of the automatic labeling. The Qanadli indices are determined using the visually graded emboli together with the original labeling or the automatic labeling; see Table 2. Table 3 shows a conversion of this index measure to a percentage of vascular obstruction.

Table 1.. The Qanadli indices determined using visually graded emboli and different tree labels (the true labels and the automatically obtained labels using the basic and multi-phase approach), deviations are indicated gray

labeling method		dataset									
		A	B	C	D	E	F	G	H	I	J
manual		0	27	1	0	26	0	1	14	7	30
automatic	basic	0	27	1	0	26	0	1	14	8	31
	multi-phase	0	27	1	0	26	0	1	14	8	29

Table 2.. Vascular obstruction (percentage), using the results from Table 1.

labeling method		dataset									
		A	B	C	D	E	F	G	H	I	J
manual		0.0%	67.5%	2.5%	0.0%	65.0%	0.0%	2.5%	35.0%	17.5%	75.0%
automatic	basic	0.0%	67.5%	2.5%	0.0%	65.0%	0.0%	2.5%	35.0%	20.0%	77.5%
	multi-phase	0.0%	67.5%	2.5%	0.0%	65.0%	0.0%	2.5%	35.0%	20.0%	72.5%

4.4 Sampling grid resolutions

As mentioned in the results sections, the reference positions have been calculated using a discretized grid of 20x20x20 voxels. We here present the dependence of the labeling accuracy on using different sampling grid sizes. In Fig. 12 (A), the labeling accuracy as a function of the grid size is shown. The speed of the determination of the reference positions is strongly influenced by the sampling resolution. Fig. 12 (B) shows the required time in hours to calculate the reference

positions using the Matlab implementation of the proposed method on a Windows 2000, Pentium IV, 2.53 GHz, 1 GB RAM computer. After the determination of the reference positions, the average required time to label a datasets is approximately 30 seconds, and is independent of the used grid size.

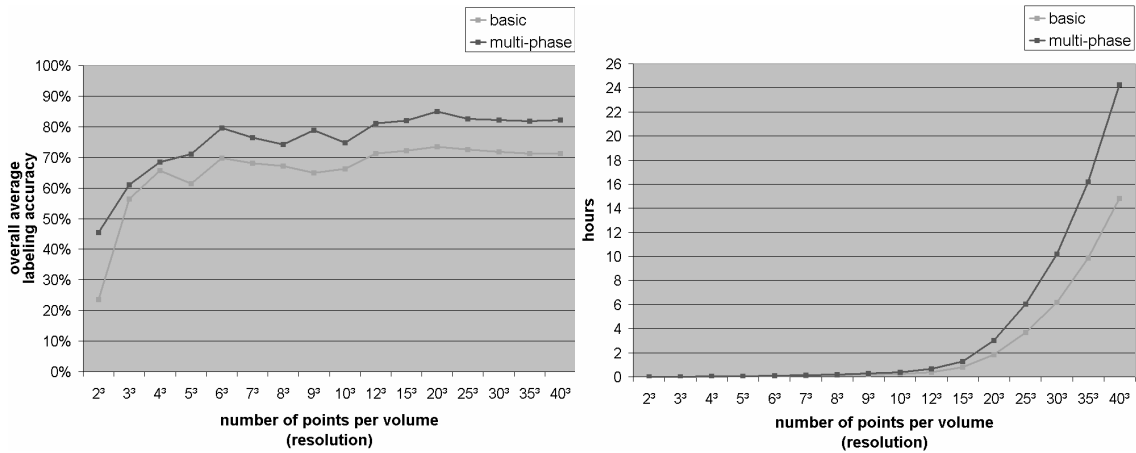


Fig. 12. (A) Average labeling accuracy for various sampling grid sizes for the training of the reference positions. (B) Calculation time for training the reference positions for 10 datasets (in hours) using volumes having different sampling grid sizes.

5. DISCUSSION

We presented an automated method for labeling the pulmonary arterial tree, which is a required step for automating the quantification of Pulmonary Embolism (PE) using the Qanadli index. This method uses reference positions that indicate the location of the peripheral branches of the arterial segments. We have presented a method to determine reference positions using manually labeled datasets.

We validated our labeling approach using binary representations of 10 arterial trees with on average approximately 900 nodes each. This validation approach was rather time consuming; the required time to create one binary tree was about 2 days.

5.1 Labeling accuracy

We first tested the accuracy of the labeling algorithm itself by using a set of “ideal” reference positions that are determined from the same dataset. In this way, the labeling accuracy is not influenced by the reference point determination that is determined using patient data with a different anatomy. The labeling approach using reference positions determined from the same dataset leads to a high accuracy, as expected. This means that the labeling algorithm is suitable for labeling the pulmonary artery tree and that errors in the labeling result from the incorrect positioning of the reference points. 100% percentage accuracy is not always obtained since our labeling approach uses a single reference position per arterial segment, and the labeling algorithm assumes that an arterial segment has a single common trunk. In practice, a segment can have more than one branch. Table 3 shows that several patients have arterial segments with more than one branch and thus not sharing a common trunk.

Table 3. Presence of common trunks in the 10 datasets for the left (L01, L02, etc.) and right (R01, R02, etc.) arterial segments

	Dataset									
	A	B	C	D	E	F	G	H	I	J
segments having more than one branch	L06, L09	L05, L06, R02	L03, R03	R03, R06	L06	R05	-	R02	-	L06

The leave-one-out tests show that the fully automated labeling approach lead to accurate labeling of the trees. Using the proposed basic approach of labeling the arterial tree, the average percentage correctly labeled nodes is 73.5% with a standard deviation of 9.4% for the 10 datasets (see Fig. 10). The proposed multi-phase labeling approach assumes a normal anatomy in the sense that common trunks occur in the lower parts of the arterial tree (for the lower segments 7, 8,

9, and 10, for the lower anterior segments 7 and 8, and for the lower posterior segments 9 and 10). The accuracy of the labeling significantly increases when a normal branching topology in the lower segments is present. The average percentage correctly labeled arterial segments using the multi-phase approach is 84.9% with a standard deviation of 10.4% (Fig. 10). The absence of these common trunks in dataset F, which is shown in Table 4, explains the relatively poor labeling results for this dataset.

Table 4. Presence of common trunks at specific arterial segment groups (“x” indicates presence; “-” indicates absence).

	Dataset									
	A	B	C	D	E	F	G	H	I	J
R07-R08	x	x	X	x	x	-	x	x	x	-
R09-R10	x	-	X	-	x	x	x	x	x	-
R07-R10	x	x	X	x	x	x	x	x	x	x
L07-L08	x	x	X	x	x	-	x	x	x	x
L09-L10	x	x	X	x	x	-	x	x	x	x
L07-L10	x	x	x	x	x	-	x	x	x	x

We construct reference positions from the manually labeled data and place these positions into a new dataset. In the ideal case, all reference positions are placed such that the closest vertex is actually part of the particular sub-tree corresponding to the reference position label. However, sometimes abnormal tree structures cause inaccurate labeling. For example, in datasets D and H, the peripheral parts of the lower arterial segments are hardly recognizable because of atelectasis, which explains the poor labeling results in dataset D and H in Fig. 10. Although these abnormal tree structures can lead to incorrect labeling, they do not deteriorate the determination of the reference points. Excluding some specific abnormal datasets, like dataset D or H, showed no significant improvements in the labeling.

We hypothesized that for labeling the arterial tree most relevant information on the position of the arterial segments can be found in peripheral parts of the tree. To test this hypothesis, we determined the accuracy on the same datasets with the positions of peripheral branches excluded. Without including the peripheral information of the tree, the accuracy dropped from 73.5% to 59.3% for the basic approach and from 84.9% to 62.8% for the multi-phase approach (Fig. 11). The significantly higher accuracy obtained with the inclusion of the peripheral part of the tree indicate, that our proposed method is able to successfully exploit the positions of the peripheral branches. Supported by the fact that arterial segment definitions are based on the position of peripheral branches, we can conclude that a bottom-up approach including peripheral segments of the arterial tree is more successful in the labeling of arterial segments.

We used the automatic labeling for the calculation of the Qanadli indices. It is shown that the errors in labeling have a minor effect on the calculation of the Qanadli index. The labeling errors commonly occur in distal branches and have no effect on the Qanadli index for emboli present in the proximal parts of the tree. Overall, the Qanadli score using the automatic labeling strongly resembles the manual scoring; for two patients the index deviates with a score of 1, that is 2.5% difference in vascular obstruction.

It has been shown that the resolution of the grid sampling used for the calculation of the reference positions, influences the accuracy of the labeling (Fig. 12). We can conclude that the accuracy increases with increasing grid size up to a size of 20x20x20, at which the accuracy is constant. The calculation times increase with order n^3 , with n the number of sample points in one direction. We have used a grid size of 20x20x20 points per volume because this produced the best labeling accuracy within an acceptable training time of 18 minutes per dataset (we used 10 datasets so therefore 3 hours training time was required). It should be noted that the construction of the model by the determination of the reference positions only has to be performed once. The labeling itself is performed in approximately 30 seconds.

5.2 Fully automated PE quantification

The presented labeling of the pulmonary arterial tree is one of the steps that is required for the fully automated quantification of PE. The fully automated approach also requires arterial tree segmentation, PE detection, and quantification of the degree of obstruction. Although some issues are still open in these fields, this study has shown that the here presented labeling approach is suitable for implementation in such a PE quantification tool.

6. CONCLUSION

We have presented an automatic method for labeling the pulmonary arterial tree for the automatic quantification of PE in CT images. The multi-phase labeling method results in an accuracy of 85%. It has been shown that labeling errors have

minor effect on the calculation of the Qanadli indices. Only two out of ten datasets had a deviation of 1 point in the Qanadli score. The presented results support the hypothesis that most information can be found in the peripheral parts of the pulmonary arterial tree. Because the presented labeling method exploits this fact it is robust to anatomical variations.

REFERENCES

1. Remy-Jardin, M., Mastora, I., and Remy, J., "Pulmonary embolus imaging with multislice CT," *Radiol.Clin.North Am.*, vol. 41, no. 3, pp. 507-519, May2003.
2. Wu, A. S., Pezzullo, J. A., Cronan, J. J., Hou, D. D., and Mayo-Smith, W. W., "CT pulmonary angiography: quantification of pulmonary embolus as a predictor of patient outcome--initial experience," *Radiology*, vol. 230, no. 3, pp. 831-835, Mar.2004.
3. Qanadli, S. D., El Hajjam, M., Vieillard-Baron, A., Joseph, T., Mesurole, B., Oliva, V. L., Barre, O., Bruckert, F., Dubourg, O., and Lacombe, P., "New CT index to quantify arterial obstruction in pulmonary embolism: comparison with angiographic index and echocardiography," *AJR Am.J.Roentgenol.*, vol. 176, no. 6, pp. 1415-1420, June2001.
4. Remy-Jardin, M., Remy, J., Mayo, J. R., and Müller, N. R., "Anatomy and Normal Variants," *CT Angiography of the Chest* 1st ed. Lippincott Williams & Wilkins, 2001, pp. 15-28.
5. Masutani, Y., MacMahon, H., and Doi, K., "Computerized detection of pulmonary embolism in spiral CT angiography based on volumetric image analysis," *IEEE Trans.Med.Imaging*, vol. 21, no. 12, pp. 1517-1523, Dec.2002.
6. Bouma, H., Vilanova, A., Quist, M. J., and Gerritsen, F. A., "Features for the Automatic Detection of Pulmonary Embolism in Contrast-Enhanced CT images," *Proceedings ASCI 2004 Port Zeelande, Ouddorp, Netherlands*, pp. 269-274, 2004.
7. Pichon, E., Novak, C. L., Kiraly, A. P., and Naidich, D. P., "A novel method for pulmonary emboli visualization from high-resolution CT images," *Proceedings of the SPIE Conference on Medical Imaging*, vol. 5367 pp. 161-170, June2004.
8. Kirbas, C. and Quek, F., "A review of vessel extraction techniques and algorithms," *ACM Computing Surveys*, vol. 36, no. 2, pp. 81-121, June2004.
9. Sebbe, R., Gosselin, B., Coche, E., and Macq, B., "Pulmonary Arteries Segmentation and Feature Extraction through Slice Marching," *Proc.ProRISC workshop on Circuits, Systems and Signal Processing*, 2003.
10. Kiraly, A. P., Pichon, E., Naidich, D. P., and Novak, C. L., "Analysis of arterial sub-trees affected by Pulmonary Emboli," *Proceedings of SPIE*, vol. 5370 2004.
11. Sonnemans, Jeroen, "Pulmonary artery/vein separation in multi-detector chest CT (Master's thesis)." Technische Universiteit Eindhoven, Department of Biomedical Engineering, 2005.
12. Pisupati, C., Wollf, L., Mitzner, W., and Zerhouni, E., "Tracking 3-D Pulmonary Tree Volumes," *Proceedings IEEE Workshop on Mathematical Methods in Biomedical Image Analysis, San Francisco, CA*, pp. 160-169, June1996.
13. Pisupati, C., Wollf, L., Mitzner, W., and Zerhouni, E., "A Central Axis Algorithm for 3D Bronchial Tree Structures," *IEEE International Symposium on Computer Vision, Miami, FL*, pp. 259-64, 1995.
14. Toroczka, Z., "Topological classification of binary trees using the Horton-Strahler index," *Phys.Rev.E.Stat.Nonlin.Soft.Matter Phys.*, vol. 65, no. 1 Pt 2, pp. 016130, Jan.2002.
15. Horton, R. E., "Erosioned development of streams and their drainage basins, hydrophysical approach to quantitative morphology," *Geological Society of America Bulletin*, vol. 56 pp. 275-370, 1945.
16. Strahler, A. N., "Hypsometric analysis of erosional topography," *Geological Society of America Bulletin*, vol. 63 pp. 1117-42, 1952.